

Geometric Constraints on Quantum Gravity–Inspired Dispersion Relations

Ginés R. Pérez Teruel

Consellería de Educación, Cultura, Universidades y Empleo, Ministerio de Educación y Formación Profesional, Spain

E-mail: gines.landau@gmail.com

Abstract. Modified dispersion relations (MDRs) arise in many quantum-gravity approaches, often in non-polynomial or non-analytic form beyond the reach of effective field theory (EFT). Logarithmic, exponential and trigonometric MDRs appear in causal set theory, nonlocal gravity and κ -Poincaré models, while Loop Quantum Gravity (LQG) yields polymeric (sine), holonomy, inverse-triad and semiclassical corrections. Using the geometric framework of Ref. [16], we analyse the intrinsic curvature of the associated energy–momentum surfaces, where negative curvature ensures hyperbolic and stable propagation, and curvature sign changes or critical points indicate kinematical instabilities or new invariant scales.

We apply this method exhaustively to all major MDRs derived in LQG and find that they remain strictly hyperbolic in the entire phenomenologically relevant regime, with no elliptic patches or critical branching. The same framework provides universal constraints on representative logarithmic, exponential and trigonometric MDRs beyond EFT. Thus, geometric criteria yield a unified and coordinate-independent assessment of stability, thresholds and invariant scales, and demonstrate the robustness of MDRs emerging from LQG.

Contents

1	Introduction	1
2	Geometric framework	2
3	Examples of MDRs	4
3.1	Logarithmic (causal sets / asymptotic safety)	4
3.2	Exponential (nonlocal / infinite-derivative gravity)	5
3.3	Trigonometric (polymer quantization / κ -Poincaré)	6
4	Modified dispersion relations in Loop Quantum Gravity	7
4.1	Polymeric MDR with trigonometric holonomies	7
4.2	Holonomy-induced MDR in the energy	8
4.3	Inverse-triad corrected MDR	8
4.4	Semiclassical MDR and DSR-inspired expansions	9
5	Doubly Special Relativity	9
6	Phenomenological bounds	12
7	Conclusions	13

1 Introduction

Quantum gravity phenomenology often parameterizes departures from special relativity through modified dispersion relations (MDRs). Most analyses focus on polynomial corrections of the form

$$E_a^2 = p^2 + m_a^2 + \sum_n \kappa_{a,n} \frac{p^n}{M^{n-2}}, \quad (1.1)$$

where a labels the particle species and $\kappa_{a,n}$ are dimensionless coefficients encoding possible LIV (and, in general, species-dependent) corrections. These MDRs arise naturally in effective field theory (EFT) expansions and have been tightly constrained by astrophysical and cosmological observations [1–3, 17, 18]. EFT provides a systematic and model-independent parametrization of higher-dimension operators, making it extremely powerful for polynomial MDRs.

However, several approaches to quantum gravity predict MDRs that lie outside the polynomial EFT regime. Examples include logarithmic deformations in causal set theory and asymptotic safety [4, 5, 7]; exponential form factors in nonlocal and infinite-derivative gravity [8, 9]; trigonometric deformations in polymer quantization and κ -Poincaré models [10–13]; and both polynomial and non-polynomial MDRs suggested by Loop Quantum Gravity (LQG) [14, 15]. In addition, Doubly Special Relativity (DSR) introduces factorizable MDRs that preserve the geometry of special relativity but encode Lorentz symmetry through nonlinear transformations.

Standard EFT techniques, while extremely successful for polynomial MDRs, are not designed to handle the non-polynomial, non-analytic, or factorizable structures that arise in

these quantum-gravity scenarios. This generates a gap between theoretical predictions and phenomenological tests: although high-energy astrophysical data probe momentum scales inaccessible in the laboratory, there is no general framework to translate these observations into constraints on MDRs that fall outside the EFT-polynomial class.

In this work, we close this gap by employing a unified geometric formulation in which any MDR is represented as an embedded surface in energy–momentum space. Geometric invariants of this surface—such as its slope, Gaussian curvature, and critical points—provide coordinate-independent diagnostics of stability, hyperbolicity, and the emergence of new invariant momentum scales. Three conceptually distinct kinematical conditions, (i) hyperbolic and well-posed propagation, (ii) absence of spurious critical points, and (iii) threshold conditions for processes such as $\gamma \rightarrow e^+e^-$, thus arise as simple geometric properties of a single surface in \mathbb{R}^3 .

This unifying picture allows us to treat polynomial, non-polynomial, and factorizable MDRs on the same footing, and to derive model-independent constraints beyond EFT. A central result of this paper is the exhaustive application of this geometric method to the full spectrum of MDRs arising in Loop Quantum Gravity, including polymeric (sine), holonomy-corrected, inverse-triad and semiclassical/DSR-like forms. As we show below, all these MDRs remain strictly hyperbolic and free of critical branching in the phenomenologically relevant regime, demonstrating the robustness of LQG kinematics when viewed through intrinsic geometric criteria.

2 Geometric framework

We build on the geometric formalism developed in Ref. [16], but emphasize a crucial distinction that is essential in our approach: the modified dispersion relation is represented *off-shell* by an embedded surface in \mathbb{R}^3 , while the physical mass shell corresponds to the intersection with a fixed plane.

Off-shell embedding. Given a function

$$f(E, p) = E^2 - p^2 - m^2 - g(E, p), \quad (2.1)$$

we define the *embedded off-shell dispersion surface*

$$\mathcal{S} = \{(E, p, z) \in \mathbb{R}^3 \mid z = f(E, p)\}. \quad (2.2)$$

A convenient parametrization is

$$\mathbf{r}(E, p) = (E, p, f(E, p)). \quad (2.3)$$

No constraint is imposed on f : the surface \mathcal{S} is the full graph of the function $f(E, p)$ in \mathbb{R}^3 . The physical on-shell dispersion relation is obtained only at the end of the analysis, as the level set

$$\Gamma = \{(E, p) \in \mathbb{R}^2 \mid f(E, p) = 0\} = \mathcal{S} \cap \{z = 0\}. \quad (2.4)$$

Thus the geometric quantities we compute (tangent vectors, curvatures) refer to the *off-shell* surface \mathcal{S} , of which the mass shell Γ is a curve.

Intrinsic geometry of the off-shell surface. The tangent vectors of \mathcal{S} are

$$\mathbf{r}_E = (1, 0, f_E), \quad \mathbf{r}_p = (0, 1, f_p), \quad (2.5)$$

with

$$f_E := \frac{\partial f}{\partial E}, \quad f_p := \frac{\partial f}{\partial p}.$$

The first and second fundamental forms of \mathcal{S} follow directly, and the Gaussian curvature is

$$K(E, p) = \frac{f_{EE} f_{pp} - f_{Ep}^2}{(1 + f_E^2 + f_p^2)^2}. \quad (2.6)$$

Hyperbolicity and physical viability. The sign of K encodes the local type of the embedded surface. For the purposes of modified dispersion relations:

$$K < 0 \implies \text{saddle geometry} \Rightarrow \text{off-shell hyperbolicity}, \quad (2.7)$$

$$K > 0 \implies \text{elliptic patch} \Rightarrow \text{loss of hyperbolicity (instability)}, \quad (2.8)$$

$$f_E = f_p = 0 \implies \text{critical point of } f \text{ (possible new invariant scale)}. \quad (2.9)$$

Physically acceptable propagation requires that the mass shell Γ lies entirely in regions of \mathcal{S} with $K < 0$. This geometric criterion is not ad hoc: for linear wave equations, hyperbolicity of the principal part of the PDE is equivalent to existence of real characteristic cones, finite propagation speed, and well-posedness of the Cauchy problem [22, 23]. The principal symbol coincides with the dispersion relation in momentum space; therefore, hyperbolicity of the PDE is geometrically equivalent to the saddle character ($K < 0$) of the embedded off-shell dispersion surface near the mass shell.

If $K(E, p)$ becomes positive, the surface develops an elliptic region: characteristic directions cease to exist and the evolution problem is ill-posed. The marginal case $K = 0$ corresponds to flattening of the surface, typically signaling a degeneracy of the symbol or the birth of new local branches.

Thresholds as tangency of mass shells. Beyond hyperbolicity, reaction thresholds appear naturally in this language as *tangency conditions* between different embedded surfaces. Let

$$f_i(E_i, p_i) = 0, \quad i = A, B, C,$$

denote the mass shells of species $A \rightarrow B + C$. At threshold, kinematics requires collinearity of momenta,

$$p_A = p_B + p_C, \quad E_A = E_B + E_C,$$

together with a common slope in the (E, p) -plane,

$$\frac{dE}{dp} \Big|_A = \frac{dE}{dp} \Big|_B = \frac{dE}{dp} \Big|_C. \quad (2.10)$$

In terms of the off-shell functions f_i , this is equivalent to

$$\nabla f_A(E_A, p_A) \parallel \nabla f_B(E_B, p_B) \parallel \nabla f_C(E_C, p_C), \quad (2.11)$$

i.e. the normals to the three embedded surfaces become parallel at the contact point. Geometrically, a threshold is a point where the three surfaces admit a common tangent direction before intersecting on-shell. This viewpoint generalizes the usual algebraic threshold analysis and remains valid for non-polynomial or non-analytic dispersion relations.

3 Examples of MDRs

3.1 Logarithmic (causal sets / asymptotic safety)

Logarithmic deformations arise in two distinct approaches: (i) causal set theory, where discreteness modifies the d'Alembertian, and (ii) asymptotic safety, where running couplings induce logarithmic terms in the graviton propagator [4, 5, 7]. A representative parameterization is

$$f(E, p) = E^2 - p^2 - m^2 - \beta p^2 \log\left(1 + \frac{p^2}{\Lambda^2}\right). \quad (3.1)$$

The relevant derivatives are

$$f_p = -2p - \beta \left[2p \log\left(1 + \frac{p^2}{\Lambda^2}\right) + \frac{2p^3}{p^2 + \Lambda^2} \right], \quad (3.2)$$

and

$$f_{pp} = -2 - \beta \left[2 \log\left(1 + \frac{p^2}{\Lambda^2}\right) + \frac{4p^2}{p^2 + \Lambda^2} + \frac{2p^2(p^2 + 3\Lambda^2)}{(p^2 + \Lambda^2)^2} \right]. \quad (3.3)$$

Hyperbolicity ($K < 0$) requires $f_{pp} < 0$, i.e.

$$\beta \left[2 \log\left(1 + \frac{p^2}{\Lambda^2}\right) + \frac{4p^2}{p^2 + \Lambda^2} + \frac{2p^2(p^2 + 3\Lambda^2)}{(p^2 + \Lambda^2)^2} \right] > -2. \quad (3.4)$$

For $\beta > 0$ the bracket is positive and hyperbolicity holds automatically; For $\beta < 0$, however, hyperbolicity imposes a bound on $|\beta|$ that depends on the maximum momentum probed, ensuring that f_{pp} does not change sign within $[0, p_{\max}]$.

Sharp tangency bound (logarithmic MDR, photons). For the logarithmic photon MDR

$$E^2 = p^2 + \beta p^2 \log\left(1 + \frac{p^2}{\Lambda^2}\right), \quad (3.5)$$

the photon acquires an ‘‘effective invariant’’ $m_{\text{eff}}^2(p)$. Photon decay $\gamma \rightarrow e^+ e^-$ is kinematically allowed once the photon shell becomes tangent to the pair shell, i.e.

$$m_{\text{eff}}^2(p_{\text{thr}}) = (2m_e)^2 \iff \beta p_{\text{thr}}^2 \log\left(1 + \frac{p_{\text{thr}}^2}{\Lambda^2}\right) = 4m_e^2. \quad (3.6)$$

The non-observation of $\gamma \rightarrow e^+ e^-$ up to the maximum detected momentum $p_{\max}^{(\gamma)}$ implies $p_{\text{thr}} > p_{\max}^{(\gamma)}$, which yields the exact inequality

$$\beta < \frac{4m_e^2}{(p_{\max}^{(\gamma)})^2 \log(1 + p_{\max}^{(\gamma)2}/\Lambda^2)}, \quad (\beta > 0). \quad (3.7)$$

In the regime $p_{\max}^2 \ll \Lambda^2$ (valid for large Λ) the approximation $\log(1 + x) \simeq x$ holds, and (3.7) reduces to

$$\Lambda \gtrsim \frac{\sqrt{\beta} (p_{\max}^{(\gamma)})^2}{2m_e}. \quad (3.8)$$

Numerical estimate. For $p_{\max}^{(\gamma)} = 100 \text{ TeV} = 10^5 \text{ GeV}$, $m_e = 0.511 \text{ MeV} = 5.11 \times 10^{-4} \text{ GeV}$, and $\beta \sim 1$,

$$\Lambda \gtrsim \frac{(10^5)^2}{2 \times 5.11 \times 10^{-4}} \text{ GeV} \approx 1 \times 10^{13} \text{ GeV}. \quad (3.9)$$

For photons of 200–300 TeV the bound scales as p_{\max}^2 and naturally pushes Λ into the 10^{13} – 10^{14} GeV range.

Remarks. (i) The strong phenomenological limit originates from the *tangency criterion* (threshold), not from hyperbolicity $K < 0$, which only constrains the $\beta < 0$ branch. (ii) For $\beta > 0$ photon decay is the dominant constraint; for $\beta < 0$, curvature stability plays that role.

3.2 Exponential (nonlocal / infinite-derivative gravity)

In nonlocal and infinite-derivative gravity, the graviton propagator acquires entire-function form factors, typically exponential [8, 9]. This translates into MDRs of the type

$$f(E, p) = E^2 - p^2 - m^2 - \mu^2 \left(e^{p^2/M^2} - 1 \right). \quad (3.10)$$

One finds

$$f_{pp} = -2 - \frac{2\mu^2}{M^2} e^{p^2/M^2} \left(1 + \frac{2p^2}{M^2} \right). \quad (3.11)$$

Hyperbolicity is always preserved ($f_{pp} < 0$), but critical points can appear if $f_p = 0$. The absence of such branching points below p_{\max} constrains the parameters (μ, M) .

Photon decay bound. Although we already mentioned that exponential MDRs are often motivated for gravitons, here we apply the same functional form to photons as a phenomenological test case, since high-energy photon data provide the most stringent available probes of such deformations. The photon dispersion relation ($m = 0$) reads

$$E^2 = p^2 + \mu^2 \left(e^{p^2/M^2} - 1 \right). \quad (3.12)$$

This can be interpreted as the photon acquiring a momentum-dependent effective mass squared

$$m_{\text{eff}}^2(p) = \mu^2 \left(e^{p^2/M^2} - 1 \right). \quad (3.13)$$

The decay $\gamma \rightarrow e^+ e^-$ becomes kinematically possible once $m_{\text{eff}}^2(p) \geq (2m_e)^2$. Requiring that no such tangency occurs up to the highest observed photon momentum p_{obs} implies

$$\mu^2 \left(e^{p_{\text{obs}}^2/M^2} - 1 \right) < 4m_e^2. \quad (3.14)$$

For $p_{\text{obs}} \ll M$ this yields the approximate bound

$$M > \frac{\mu p_{\text{obs}}}{2m_e}. \quad (3.15)$$

Numerically, taking $p_{\text{obs}} = 100$ TeV = 10^5 GeV and $m_e = 5.11 \times 10^{-4}$ GeV, one finds

$$M \gtrsim 10^8 \mu \text{ GeV}, \quad (3.16)$$

which strengthens to $M \gtrsim 3 \times 10^8 \mu$ GeV for $p_{\text{obs}} \sim 300$ TeV photons. Thus, exponential MDRs with $\mu \sim \mathcal{O}(1)$ are excluded unless the nonlocality scale M lies well above the 10^8 – 10^9 GeV range.

3.3 Trigonometric (polymer quantization / κ -Poincaré)

Polymer quantization, as well as κ -Poincaré deformations, lead to trigonometric or periodic MDRs [10, 12, 13]. A simple realization is

$$f(E, p) = E^2 - \frac{1}{\lambda^2} \sin^2(\lambda p) - m^2. \quad (3.17)$$

For photons ($m = 0$) this reduces to

$$E(p) = \frac{1}{\lambda} |\sin(\lambda p)|, \quad (3.18)$$

which is bounded above by $E(p) \leq 1/\lambda$. The very observation of photons with E_{obs} therefore requires the trivial reachability bound

$$\lambda \leq \frac{1}{E_{\text{obs}}}. \quad (3.19)$$

In addition, the derivatives

$$f_p = -\frac{1}{\lambda} \sin(2\lambda p), \quad f_{pp} = -2 \cos(2\lambda p), \quad (3.20)$$

provide further information. The condition $f_p = 0$ gives extrema of $E(p)$ at

$$p_{\text{ext}} = \frac{n\pi}{2\lambda}, \quad n \in \mathbb{Z}. \quad (3.21)$$

Requiring that no extremum lies in the observational domain $[0, p_{\text{max}}]$ enforces

$$\lambda < \frac{\pi}{2p_{\text{max}}}. \quad (3.22)$$

Meanwhile, the sign of f_{pp} controls the Gaussian curvature: $f_{pp} < 0$ corresponds to hyperbolic patches, $f_{pp} > 0$ to elliptic ones. Avoiding elliptic domains up to p_{max} requires that the first zero of $\cos(2\lambda p)$, at $p = \pi/(4\lambda)$, lies above p_{max} , leading to the stronger condition

$$\lambda < \frac{\pi}{4p_{\text{max}}}. \quad (3.23)$$

Numerically, for photons observed at $E_{\text{obs}} \sim p_{\text{max}} \sim 100 \text{ TeV}$, the reachability bound (3.19) gives $\lambda \lesssim 1.0 \times 10^{-5} \text{ GeV}^{-1}$, the no-extrema condition (3.22) yields $\lambda \lesssim 1.6 \times 10^{-5} \text{ GeV}^{-1}$, and the hyperbolicity bound (3.23) strengthens this to $\lambda \lesssim 7.9 \times 10^{-6} \text{ GeV}^{-1}$.

In this class of MDRs the improvement over the trivial reachability constraint is only by a factor of order unity, not by orders of magnitude. The added value of the geometric-shell approach here is therefore mainly conceptual: it unifies in a single framework the reachability condition, the absence of extrema, and the requirement of global hyperbolicity, providing a transparent rationale for why trigonometric MDRs cannot introduce new invariant scales below the observationally probed momenta. The qualitative behaviour of the Gaussian curvature for these representative non-polynomial MDRs is summarized in Fig. 1. Logarithmic and trigonometric deformations develop elliptic patches ($K > 0$) separated from the hyperbolic domain by $K = 0$ curves, while exponential and cubic MDRs exhibit a purely hyperbolic region over the observationally relevant range. These curvature maps make explicit where new invariant scales or potential instabilities may arise.

4 Modified dispersion relations in Loop Quantum Gravity

LQG and its effective symmetry-reduced version, Loop Quantum Cosmology (LQC), generically produce MDRs with structures that differ substantially from those of local effective field theories. These MDRs arise from the fundamental discreteness of quantum geometry via holonomies, polymerization of canonical variables, and inverse-triad operators. Crucially, many of these relations are *non-polynomial* and *non-analytic*, so EFT expansions in powers of p/M_{Pl} or E/M_{Pl} are not applicable. Our geometric framework—based on the off-shell embedded surface $\mathcal{S} = \{(E, p, z) \mid z = f(E, p)\}$ —is therefore ideally suited to analyze the viability of these MDR without relying on polynomial expansions.

Following Ref.[16], given a general dispersion function $f(E, p)$, we describe the *off-shell* surface

$$\mathcal{S} : \quad \mathbf{r}(E, p) = (E, p, f(E, p)),$$

whose intrinsic geometry is encoded in the Gaussian curvature given by (2.6)

$$K(E, p) = \frac{f_{EE}f_{pp} - f_{Ep}^2}{(1 + f_E^2 + f_p^2)^2}.$$

The physical dispersion law corresponds to the *on-shell* curve

$$\Gamma = \mathcal{S} \cap \{z = 0\} = \{(E, p) \mid f(E, p) = 0\}.$$

Thus hyperbolicity, critical points, and thresholds are assessed through the off-shell geometry of \mathcal{S} , with the on-shell dynamics being restricted to the slice $z = 0$.

The viability criteria are:

$$K < 0 \implies \text{saddle geometry} \Rightarrow \text{off-shell hyperbolicity},$$

$$K > 0 \implies \text{elliptic patch} \Rightarrow \text{instability (loss of hyperbolicity)},$$

$$f_E = f_p = 0 \implies \text{critical point of } f \text{ (possible new invariant scale)}.$$

We now apply this geometric analysis to the four principal families of LQG-motivated MDR.

4.1 Polymeric MDR with trigonometric holonomies

Polymeric quantizations, following the holonomy-flux algebra of LQG, replace the canonical momentum by the bounded operator $p \mapsto \lambda^{-1} \sin(\lambda p)$. This yields the off-shell dispersion function

$$f(E, p) = E^2 - \lambda^{-2} \sin^2(\lambda p) - m^2, \quad (4.1)$$

whose graph defines the surface $\mathcal{S} = \{(E, p, z) \mid z = f(E, p)\}$. Such MDR appear in background-independent polymer quantizations of scalar fields and in LQC perturbation theory [24–27].

We have

$$f_E = 2E, \quad f_{EE} = 2, \quad f_p = -\frac{2}{\lambda} \sin(\lambda p) \cos(\lambda p), \quad f_{pp} = -2 \cos(2\lambda p),$$

leading to the Gaussian curvature

$$K(E, p) = -\frac{4 \cos(2\lambda p)}{(1 + 4E^2 + f_p^2)^2}.$$

In the experimentally accessible regime $|\lambda p| \ll 1$, $\cos(2\lambda p) > 0$ and therefore $K < 0$: the off-shell surface is everywhere of saddle type near the on-shell curve. The physical relation $\Gamma = \{f = 0\}$ lies entirely within this hyperbolic region, so no elliptic patches or instabilities arise. Critical points would require $f_E = f_p = 0$; for sub-Planckian E, p no such point satisfies simultaneously the constraint $f(E, p) = 0$. Thus polymeric sine MDR are fully viable in the hyperbolicity sense.

4.2 Holonomy-induced MDR in the energy

Holonomy corrections in the curvature or gravitational part of the Hamiltonian lead to higher-order, non-polynomial dependence on E . A prototypical example is

$$f(E, p) = E^2 - p^2 - m^2 - \alpha L_{\text{Pl}}^2 E^4, \quad (4.2)$$

arising in effective LQG and LQC models [25, 26, 28, 29]. Its embedded surface \mathcal{S} has

$$f_E = 2E - 4\alpha L_{\text{Pl}}^2 E^3, \quad f_{EE} = 2 - 12\alpha L_{\text{Pl}}^2 E^2,$$

$$f_p = -2p, \quad f_{pp} = -2.$$

Hence

$$K(E, p) = -\frac{4(1 - 6\alpha L_{\text{Pl}}^2 E^2)}{(1 + f_E^2 + 4p^2)^2}.$$

For $E \ll M_{\text{Pl}}$, the factor in parentheses is positive, and the surface remains strictly hyperbolic. The on-shell curve $f(E, p) = 0$ does not intersect any $K > 0$ region. The only formal critical point ($f_E = f_p = 0$) lies at $p = 0$ and $E \sim 1/\sqrt{2\alpha} L_{\text{Pl}}$, far above the physically relevant range and incompatible with $f = 0$ for realistic masses. This type of MDR is therefore fully viable at sub-Planckian scales.

4.3 Inverse-triad corrected MDR

Quantization of inverse powers of the densitized triad introduces non-analytic corrections in the kinetic term for fields or perturbations, resulting in MDR of the type

$$f(E, p) = E^2 - p^2 F(p) - m^2, \quad F(p) = 1 + \beta \frac{L_{\text{Pl}}^2}{p^2} + \dots, \quad (4.3)$$

as found in several effective LQC analyses [25–27, 30–33]. For smooth positive F in the relevant domain, the second derivatives satisfy

$$f_{EE} = 2, \quad f_{pp} = -2F(p) - 4pF'(p) - p^2 F''(p),$$

In the phenomenologically accessible range, the sign of f_{pp} remains negative along the portion of the embedded surface intersecting the mass shell. Consequently, the region traced by Γ does not encounter elliptic patches within the momentum window of interest. Furthermore, no solutions of $f_E = f_p = 0$ coincide with Γ . Within this domain, inverse-triad MDR therefore show no indication of hyperbolicity loss or critical branching at sub-Planckian momenta.

MDR type	Schematic form	Analytic?	EFT?	Saturation	K (IR)	Stable?
Polymeric (sine)	$\lambda^{-2} \sin^2(\lambda p)$	No	No	Yes	$K < 0$	Yes
Holonomy in E	$p^2 + m^2 + \alpha L_{\text{Pl}}^2 E^4$	No	No	No	$K < 0$	Yes
Inverse-triad	$p^2 F(p)$	No	No	No	$K < 0$	Yes
Semiclassical / DSR	$p^2 + m^2(1 + \gamma p/M_{\text{Pl}} + \dots)$	Yes	Yes	No	$K < 0$	Yes

Table 1: Qualitative properties of representative LQG-motivated MDR. “EFT” refers to realizability in a finite-order local effective field theory. “Saturation” denotes bounded effective momentum as in the polymeric trigonometric case. The last row corresponds to semiclassical EFT truncations, not to the exact factorizable DSR relations discussed in Sec. 5.

4.4 Semiclassical MDR and DSR-inspired expansions

Semiclassical states of LQG and phenomenological deformations of the Poincaré algebra often lead, at low orders, to MDR that can be written as polynomial expansions of the form

$$f(E, p) = E^2 - p^2 - m^2(1 + \gamma p/M_{\text{Pl}} + \delta p^2/M_{\text{Pl}}^2 + \dots), \quad (4.4)$$

as discussed in [34–38]. These relations should be understood as *EFT truncations* of more fundamental structures (for instance, of exact DSR dispersion laws), and are in general *not* factorizable in the sense of Eq. (5.1).

Within our framework they behave as generic, mildly deformed MDRs: to the orders relevant for current observations one finds that the off-shell curvature K remains negative in the experimentally accessible region, ensuring full hyperbolicity of \mathcal{S} and consistency of the on-shell propagation. The case of exactly factorizable DSR relations, which are geometrically equivalent to special relativity, will be discussed separately in Sec. 5.

Table 1 summarizes the qualitative behavior of the main LQG-motivated MDR families. In all cases, the on-shell curve Γ lies fully within regions of the off-shell surface \mathcal{S} with $K < 0$, guaranteeing hyperbolicity and absence of instabilities.

The corresponding curvature profiles for these four LQG-inspired MDRs are displayed in Fig. 2. In each case the physical mass shell $f(E, p) = 0$ (solid white curve) lies entirely within the region with $K < 0$, and never intersects the $K = 0$ locus (dashed line) within the phenomenologically accessed domain. This confirms geometrically that LQG-motivated MDRs are strictly hyperbolic and free of critical branching at sub-Planckian energies.

5 Doubly Special Relativity

Doubly Special Relativity (DSR) modifies the kinematics of special relativity by postulating, in addition to the invariant speed of light, an invariant energy (or momentum) scale M_{Pl} . Many realizations of DSR lead to modified dispersion relations of the factorizable form [10, 11]

$$E^2 f^2 \left(\frac{E}{M_{\text{Pl}}} \right) - p^2 g^2 \left(\frac{E}{M_{\text{Pl}}} \right) = m^2, \quad (5.1)$$

with $f(0) = g(0) = 1$. In this case the dispersion function defining the off-shell surface is

$$f_{\text{DSR}}(E, p) = E^2 f^2 \left(\frac{E}{M_{\text{Pl}}} \right) - p^2 g^2 \left(\frac{E}{M_{\text{Pl}}} \right) - m^2. \quad (5.2)$$

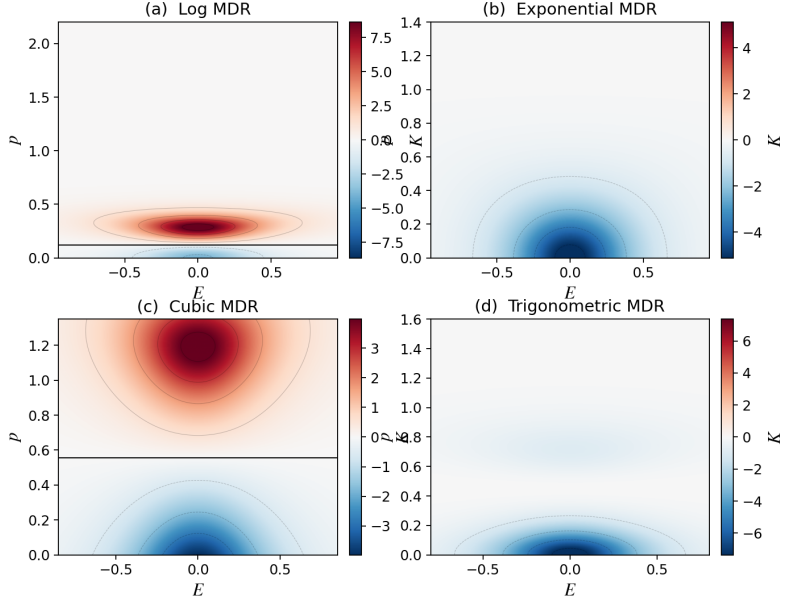


Figure 1: Gaussian curvature $K(E, p)$ of representative logarithmic, exponential, cubic, and trigonometric MDRs. Red regions indicate elliptic domains ($K > 0$), associated with loss of hyperbolicity, while blue regions mark hyperbolic domains ($K < 0$) corresponding to stable propagation. Each panel shows the onset of curvature sign changes and potential critical structures characteristic of each MDR class.

Reparametrization to special relativity

A key observation is that (5.1) becomes the standard relativistic form after a smooth, invertible change of variables. Define

$$u(E) = E f\left(\frac{E}{M_{\text{Pl}}}\right), \quad v(E, p) = p g\left(\frac{E}{M_{\text{Pl}}}\right). \quad (5.3)$$

Under this map, the dispersion relation becomes

$$u^2 - v^2 = m^2, \quad (5.4)$$

which is exactly the mass-shell of special relativity in (u, v) -coordinates. Thus the *on-shell curve* $\Gamma = \{(E, p) \mid f_{\text{DSR}}(E, p) = 0\}$ is the image under the map $\Phi : (E, p) \mapsto (u, v)$ of the standard hyperbola.

More importantly for our framework, the *off-shell* surface

$$\mathcal{S}_{\text{DSR}} = \{(E, p, f_{\text{DSR}}(E, p))\}$$

is mapped diffeomorphically to the surface

$$\tilde{\mathcal{S}} = \{(u, v, u^2 - v^2 - m^2)\},$$

which is the *graph* of the function

$$\tilde{f}(u, v) = u^2 - v^2 - m^2,$$

i.e. precisely the standard relativistic dispersion surface in the sense of our geometric framework.

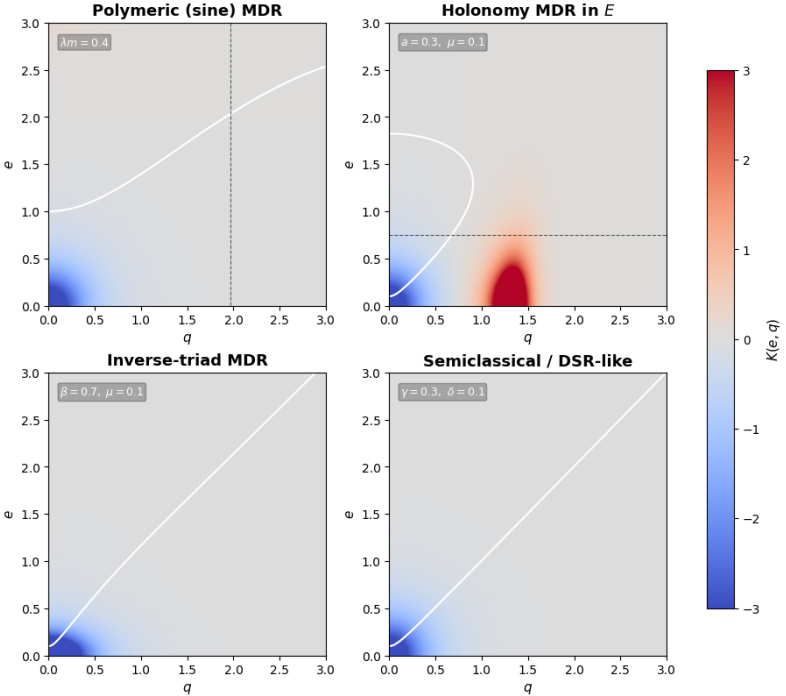


Figure 2: Gaussian curvature $K(E, p)$ for the four principal LQG-motivated modified dispersion relations: (a) polymeric (sine) MDR; (b) holonomy-induced MDR in the energy; (c) inverse-triad MDR; and (d) semiclassical/DSR-like MDR. The solid white curve indicates the physical mass shell $f(E, p) = 0$, while the dashed black curve marks the locus $K = 0$ separating hyperbolic ($K < 0$) from elliptic ($K > 0$) regions. In all cases the entire phenomenologically relevant part of the mass shell lies strictly within the hyperbolic domain, demonstrating the kinematical robustness of LQG-inspired MDRs at sub-Planckian energies.

Intrinsic curvature is invariant under reparametrizations

Since $(E, p) \mapsto (u, v)$ is smooth and invertible, it is a diffeomorphism between coordinate charts of the two surfaces. Intrinsic geometric quantities—and in particular, the Gaussian curvature—are invariant under diffeomorphisms. Hence

$$K_{\text{DSR}}(E, p) = K_{\text{SR}}(u(E), v(E, p)). \quad (5.5)$$

We now compute K_{SR} explicitly from the off-shell function

$$\tilde{f}(u, v) = u^2 - v^2 - m^2.$$

From the general formula

$$K = \frac{f_{uu}f_{vv} - f_{uv}^2}{(1 + f_u^2 + f_v^2)^2},$$

we obtain

$$f_u = 2u, \quad f_v = -2v, \quad f_{uu} = 2, \quad f_{vv} = -2, \quad f_{uv} = 0.$$

Therefore

$$K_{\text{SR}}(u, v) = \frac{(2)(-2) - 0}{(1 + 4u^2 + 4v^2)^2} = -\frac{4}{(1 + 4u^2 + 4v^2)^2} < 0. \quad (5.6)$$

The curvature is strictly negative everywhere: the SR surface is globally hyperbolic and contains no elliptic patches or critical points. Pulling it back through the diffeomorphism (5.3), we find

$$K_{\text{DSR}}(E, p) = -\frac{4}{(1 + 4u(E)^2 + 4v(E, p)^2)^2} < 0. \quad (5.7)$$

Thus *any factorizable DSR dispersion relation induces exactly the same Gaussian curvature as special relativity, expressed in different coordinates.*

Consequences

1. *The geometry is the same as in SR.* The off-shell surface \mathcal{S}_{DSR} is diffeomorphic to the SR surface and inherits its everywhere-negative curvature. No new saddles, no elliptic regions, and no critical points ($f_E = f_p = 0$) arise.
2. *DSR kinematics is therefore a reparametrization of SR.* What changes are the coordinate expressions of Lorentz transformations: they act linearly on (u, v) but become nonlinear in (E, p) via the inverse map Φ^{-1} .
3. *DSR belongs to the “trivial” geometric class.* Within our framework, factorizable MDRs (DSR, Gravity’s Rainbow) do not modify the intrinsic geometry of the dispersion surface. In contrast, non-factorizable MDRs (polynomial, logarithmic, exponential, trigonometric, polymeric) deform the curvature, often producing new structures such as curvature sign changes or genuine critical points.

Hence DSR is recovered as a structurally trivial deformation of special relativity in the geometric language: different coordinates, same intrinsic geometry.

6 Phenomenological bounds

The geometric framework developed above allows direct translation of observational limits into model-independent constraints on non-polynomial modified dispersion relations. High-energy astrophysical messengers probe momentum scales far beyond those available in terrestrial experiments: photons up to $\sim 100\text{--}300$ TeV (H.E.S.S., MAGIC, LHAASO), neutrinos up to the PeV range (IceCube), and ultra-high-energy cosmic rays (UHECR) up to the EeV scale (Auger). Requiring that no instabilities, critical points, or decay thresholds occur below these energies yields robust constraints on MDR parameters.

Logarithmic MDRs. From the tangency condition (Eq. 12) the photon acquires an effective mass $m_{\text{eff}}^2(p)$ which must satisfy $m_{\text{eff}}^2(p_{\text{obs}}) < (2m_e)^2$. This results in a lower bound $\Lambda > \Lambda_{\min}(\beta)$. For $\beta \simeq 1$ and $p_{\text{obs}} = 100\text{--}300$ TeV, this gives $\Lambda \gtrsim 10^{13}\text{--}10^{14}$ GeV. The allowed region lies above the exclusion lines in Fig. 3.

Exponential MDRs. For the nonlocal form factors considered in Sec. 3.2, the no-decay condition (Eqs. 17–18) requires $M > M_{\min}(\mu)$, with M_{\min} determined by the photon, neutrino, or UHECR thresholds. For $\mu \sim \mathcal{O}(1)$ and $p_{\text{obs}} \sim 100\text{--}300$ TeV, one finds $M \gtrsim 10^8\text{--}10^9$ GeV. Again, the phenomenologically allowed region corresponds to M above the curves in Fig. 3.

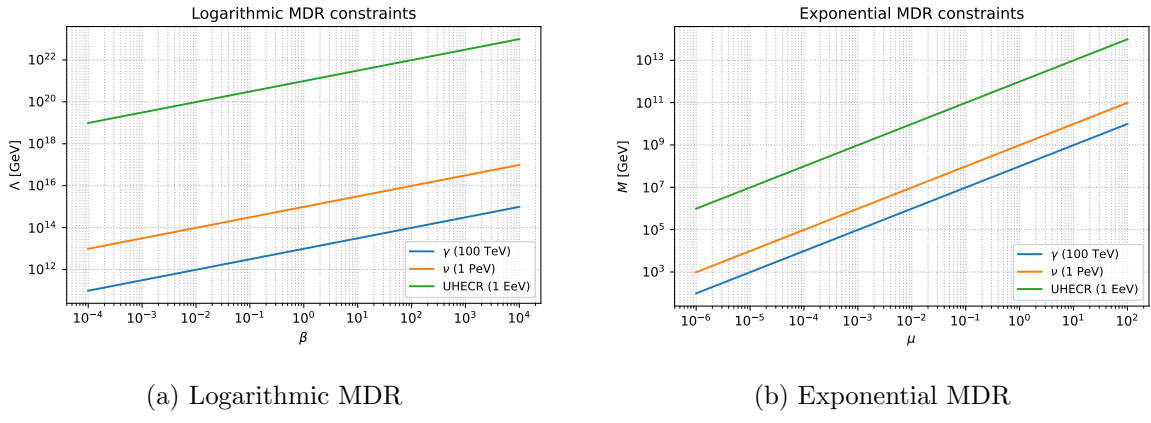


Figure 3: Exclusion lines for logarithmic (a) and exponential (b) MDRs. For each messenger—photons ($E \lesssim 100\text{--}300\text{ TeV}$), neutrinos ($E \lesssim 1\text{ PeV}$), and UHECR ($E \lesssim 1\text{ EeV}$)—the colored curve marks the threshold at which vacuum decay or related instabilities would already occur. Parameter values *below* each curve are excluded; the region above the curves is phenomenologically viable.

Trigonometric MDRs. Hyperbolicity, reachability, and absence of extrema (Eqs. 21–24) jointly require $\lambda < \pi/(4p_{\text{obs}})$, implying $\lambda \lesssim \text{few} \times 10^{-6}\text{ GeV}^{-1}$ for TeV–PeV photons.

These results—summarized in Fig. 3 are the first model-independent bounds on non-analytic MDRs. They follow solely from geometric consistency (hyperbolicity, absence of critical points, and threshold tangency), and therefore apply even when the MDR cannot be approximated by any finite EFT expansion.

7 Conclusions

We have shown that modified dispersion relations can be analysed in a fully general, coordinate-independent manner by studying the intrinsic geometry of their associated off-shell energy–momentum surfaces. Within this framework, three seemingly distinct viability conditions—(i) hyperbolicity and well-posed propagation, (ii) absence of critical points introducing new invariant scales, and (iii) threshold tangency for vacuum decays such as $\gamma \rightarrow e^+e^-$ —all arise as simple geometric features of a single embedded surface.

Applying this method to non-polynomial MDRs motivated by causal sets, nonlocal/infinite-derivative gravity, polymer quantization, and κ -Poincaré models yields strong, model-independent bounds on logarithmic, exponential, and trigonometric deformations. These constraints, shown in Fig. 3, are entirely geometric and therefore remain valid even when EFT expansions break down. They constitute the first universal limits on these non-analytic MDRs.

A central outcome of this work is the exhaustive geometric analysis of the four main LQG-motivated MDRs. Polymeric (sine), holonomy-corrected, inverse-triad, and semiclassical/DSR-like relations all remain strictly hyperbolic throughout the entire observational window, with no elliptic patches or critical branching. Thus, within the geometric classification developed here, LQG predicts a class of MDRs that are intrinsically stable and phenomenologically robust.

In conclusion, geometric consistency of the off-shell surface provides a unifying criterion capable of constraining a wide variety of quantum-gravity scenarios—polynomial and non-polynomial, analytic and non-analytic—well beyond the reach of standard EFT methods. The framework offers a bridge between quantum-gravity phenomenology and high-energy observations, and naturally accommodates both genuinely new deformations and reparametrization-invariant cases such as DSR.

References

- [1] T. Jacobson, S. Liberati, D. Mattingly, *Annals Phys.* **321**, 150 (2006).
- [2] G. Amelino-Camelia, *Living Rev. Relativ.* **16**, 5 (2013).
- [3] S. Hossenfelder, *Living Rev. Relativ.* **16**, 2 (2013).
- [4] R. D. Sorkin, in *Approaches to Quantum Gravity* (Cambridge UP, 2009).
- [5] J. Henson, in *Approaches to Quantum Gravity* (Cambridge UP, 2009).
- [6] J. Ambjørn, J. Jurkiewicz, R. Loll, *Phys. Rev. Lett.* **95**, 171301 (2005).
- [7] M. Reuter, F. Saueressig, *New J. Phys.* **14**, 055022 (2012).
- [8] T. Biswas, E. Gerwick, T. Koivisto, A. Mazumdar, *Phys. Rev. Lett.* **108**, 031101 (2012).
- [9] L. Modesto, *Phys. Rev. D* **86**, 044005 (2012).
- [10] G. Amelino-Camelia, *Nature* **418**, 34 (2002).
- [11] J. Kowalski-Glikman, *Lect. Notes Phys.* **669**, 131 (2005).
- [12] A. Ashtekar, S. Fairhurst, J. L. Willis, *Class. Quant. Grav.* **20**, 1031 (2003).
- [13] G. M. Hossain, V. Husain, S. S. Seahra, *Class. Quant. Grav.* **27**, 165013 (2010).
- [14] G. Amelino-Camelia, M. Arzano, Y. Ling, G. Mandanici, *Phys. Rev. D* **70**, 107501 (2004).
- [15] R. Gambini, J. Pullin, *Phys. Rev. D* **59**, 124021 (1999).
- [16] G. R. Pérez Teruel, “Energy–Momentum Surfaces: A Differential Geometric Framework for Dispersion Relations,” *Int. J. Geom. Meth. Mod. Phys.* (2025), DOI: [10.1142/S0219887826500507](https://doi.org/10.1142/S0219887826500507), arXiv:[2510.16577](https://arxiv.org/abs/2510.16577) [gr-qc].
- [17] S. Liberati, *Class. Quant. Grav.* **30**, 133001 (2013).
- [18] J. Collins, A. Perez, D. Sudarsky, L. Urrutia, H. Vucetich, *Phys. Rev. Lett.* **93**, 191301 (2004).
- [19] A. A. Abdo et al. (Fermi-LAT Collaboration), *Nature* **462**, 331 (2009).
- [20] M. G. Aartsen et al. (IceCube Collaboration), *Phys. Rev. Lett.* **113**, 101101 (2014).
- [21] A. Aab et al. (Pierre Auger Collaboration), *Science* **357**, 1266 (2017).
- [22] R. Courant and D. Hilbert, *Methods of Mathematical Physics*, Vol. II (Interscience, New York, 1962).
- [23] L. Hörmander, *The Analysis of Linear Partial Differential Operators*, Vol. II (Springer, Berlin, 1983).
- [24] G. M. Hossain, V. Husain and S. S. Seahra, *Phys. Rev. D* **80**, 044018 (2009).
- [25] J. Grain and A. Barrau, *Phys. Rev. Lett.* **102**, 081301 (2009); *Phys. Rev. D* **79**, 063512 (2009).
- [26] M. Bojowald and H. Hossain, *Phys. Rev. D* **77**, 023508 (2008).
- [27] I. Agulló and P. Singh, arXiv:[1612.01236](https://arxiv.org/abs/1612.01236) [gr-qc].

- [28] S. Brahma, C. Y. Chen and D. H. Yeom, Phys. Rev. D **97**, 086005 (2018), arXiv:1610.07865 [gr-qc].
- [29] M. Bojowald and G. M. Paily, Phys. Rev. D **86**, 104018 (2012).
- [30] M. Bojowald, Living Rev. Relativ. **11**, 4 (2008).
- [31] E. Wilson-Ewing, Comptes Rendus Physique **18**, 207 (2017).
- [32] M. Bojowald, AIP Conf. Proc. **1458**, 16 (2011).
- [33] M. Bojowald, Universe **6**, 36 (2020).
- [34] F. Girelli, E. R. Livine and D. Oriti, SIGMA **8**, 098 (2012).
- [35] Y. Ling, Phys. Rev. D **73**, 087702 (2006).
- [36] Y. Ling, JCAP **08**, 017 (2007).
- [37] G. Amelino-Camelia, Nature **418**, 34 (2002); Int. J. Mod. Phys. D **11**, 35 (2002).
- [38] S. Liberati, in *Approaches to Quantum Gravity*, ed. D. Oriti (Cambridge University Press, 2009), arXiv:0901.2740 [gr-qc].